Research in Pharmaceutical Sciences, December 2024; 19(6): 712-728
Received: 20-08-2023
Peer Reviewed: 03-02-2024
Revised: 23-02-2024
Accepted: 28-08-2024
Published: 15-12-2024

School of Pharmacy & Pharmaceutical Sciences
Isfahan University of Medical Sciences

Original Article

Phytochemicals from *Pyrrosia longifolia* (Burm. f.) C.V. Morton with antibacterial activity

Hilwan Yuda Teruna[1], Rohimatul Khodijah[1], Neni Frimayanti[2], and Rudi Hendra[1,*]

[1]*Department of Chemistry, Faculty of Mathematics and Natural Sciences, Universitas Riau, Pekanbaru, Indonesia.*
[2]*Sekolah Tinggi Ilmu Farmasi Riau, Pekanbaru, Indonesia.*

Abstract

Background and purpose: *Pyrrosia longifolia* is one of the medicinal plants in Indonesia. However, it has received little attention regarding pharmacological properties and phytochemicals. This study aimed to isolate bioactive compounds and evaluate their antibacterial activities.
Experimental approach: The secondary metabolites were isolated using a bioassay-guided approach. The aerial part was macerated in methanol and the crude methanol was partitioned with organic solvents to obtain n-hexane, dichloromethane, ethyl acetate, and water extracts. The ethyl acetate extract was purified using chromatography procedures, yielding six chemicals, and their structures were determined using spectroscopy. The antibacterial activity of the compounds was evaluated.
Findings/Results: Six secondary phytochemical metabolites were identified including naringin (1), catechin (2), quercetin (3), rutin (4), kaempferol (5), and mangiferin (6). The absolute configurations of compounds 1 and 2 were ascertained using electronic circular dichroism as 2S for naringin and 2R, 3S for catechin. The compounds exhibited antibacterial activity against several pathogenic bacteria, with MIC and MBC values ranging from 7.8 to 250 µg/mL. Computational investigations of these compounds revealed a substantial affinity for bacterial receptors' active and allosteric regions. Furthermore, rutin exhibited the capacity to reduce the activity of β-ketoacyl-acyl carrier protein synthase III, enhancing its antibacterial effectiveness.
Conclusion and implications: The *in-vitro* assessment revealed that the six identified compounds possess a wide range of antibacterial activity, which was corroborated by *in-silico* analyses. However, further investigation is required to back up the conclusion of this study.

Keywords: Phenolic antibacterial compounds; Polypodiaceae; *Pyrrosia longifolia*; Secondary metabolites isolation; PDB ID: 2ZDQ; 1HNJ; 3IL7.

INTRODUCTION

Pyrrosia is a genus of epiphytic plants, a member of the Polypodiaceae family, consisting of approximately 69 species. The distribution, constituents, and affluence of epiphytic plants within the host tree have unique characteristics. This is closely related to the characteristics of the bark, the slope of the trunk, the branching system, and the twigs, in addition to the availability of water, temperature, humidity, and light intensity (1). The *Pyrrosia* genus is a fern whose species are widely used in traditional medicine. According to the Chinese Pharmacopoeia, the three species of *Pyrrosia* known as *P. lingua*, *P. sheareri*, and *P. petiolosa* are the primary ingredients in the traditional Chinese medicine known as "Shiwei." This medicine is used to treat a variety of conditions, including urocystitis, urinary calculus, bloody urine, coughs, and bronchitis (2,3).

Access this article online	
	Website: http://rps.mui.ac.ir
	DOI: 10.4103/RPS.RPS_151_23

*Corresponding author: R. Hendra
Tel: +62-81365340190, Fax: +62-76163272
Email: rudi.hendra@lecturer.unri.ac.id

P. lingua, P. petiolosa, P. sheareri, P. heterophylla, P. gralla, P. porosa, and *P. subfurfuracea* have been reported to possess some pharmacological properties, including antitumor, anticancer, anti-inflammatory, antiviral, antioxidant, and antibacterial properties (4-7), attributed to their compounds such as flavonoids (kaempferol, quercetin, and their glycosides), flavanone (naringenin), and xanthone (mangiferin) (8-10). On the other hand, the pharmacological properties and phytochemicals of *P. longifolia* have not yet been investigated. The leaves of this species are utilized in certain regions of Indonesia and the Pacific Islands to make a decoction that helps relieve labor-associated pains (11,12). Previous research found that the ethyl acetate extract of species had high radical scavenging activity (IC_{50} = 28.22 µg/mL) and intermediate antibacterial activity against some pathogenic bacteria. However, the phytochemicals responsible for its antibacterial properties have not yet been discovered (13,14).

In the current study, the chemical compounds including flavanols, flavanone, flavan-3-ol, and xanthone were identified from the epiphytic ferns in ethyl acetate extracts of *P. longigolia*. Furthermore, their *in-vitro* antibacterial activities were investigated, alongside an analysis of the probable mechanisms through an *in-silico* study. These analyses used computer-aided drug design tools, including molecular docking predicting the binding interaction of a prospective medicine with its target, providing critical information about the antibacterial properties of the isolated molecules (15). This comprehensive approach aimed to elucidate the effectiveness of the compounds under examination and provide insights into their interactions at the molecular level.

MATERIALS AND METHODS

General experimental procedure

UV-Vis spectra were determined using a Shidmazu UV-1800 spectrophotometer (Japan) and electronic circular dichroism (ECD) spectra were recorded on a JASCO J-1500 spectropolarimeter at 26 °C in quartz cells of 5 mm path length. Fourier transform infrared spectroscopy (FTIR) spectra were determined on a Shimadzu IR Prestige-21 spectrophotometer (Japan). Proton and carbon-13 nuclear magnetic resonance (1H and 13C NMR) spectra were recorded with a spectrometer of Agilent DD2 system operating at 500 (1H) and 125 (13C) MHz, using residual and deuterated solvent peaks as reference standards. Column chromatography was performed with silica gel 60 GF254 (230-400 mesh, Merck, Germany). Fractions were monitored by TLC silica gel GF254 (Merck, Germany).

Plant material

The aerial parts of *P. longifolia* were collected in Pekanbaru, Indonesia (0.539166o N, 101.448843o E). Prof. Fitmawati of the Department of Biology, Universitas Riau authenticated the plant. A voucher specimen (No. 185/UN19.5.1.1.3-4/EP/2021) was deposited in the Laboratory of Botany, Department of Biology, Universitas Riau.

Extraction and isolation

The air-dried and powdered aerial parts (5.0 kg) of *P. longifolia* were extracted with methanol three times under maceration, and the solvent was evaporated *in vacuo*. The crude methanol extract was partitioned in H_2O and extracted successively with n-hexane, dichloromethane, and ethyl acetate. The ethyl acetate fraction (40 g) was separated by using vacuum liquid chromatography with a silica gel column with a gradient elution of n-hexane/ethyl acetate/methanol, and eight fractions (F1-8) were obtained according to the thin-layer chromatography (TLC) monitor. The purification of the fraction was subjected based on a bioassay-guided approach and fraction 7 (2.0 g) was applied to silica gel flash liquid column chromatography (CH_2Cl_2/MeOH, 9:1 to 3:7) to obtain compounds 1 (17 mg), 2 (13 mg), 3 (37 mg), 4 (28 mg), 5 (25 mg), 6 (22 mg).

Antibacterial activity

Microbial strain

Bacillus subtilis ATCC 1965, *B. cereus* ATCC 10876, *Staphylococcus aureus* ATCC 6538, *Vibrio alginolyticus* ATCC 17749, and *Listeria monocytogenes* ATCC 7644 were used in this research. The microbial isolates were grown on agar plates at 4 °C in the Laboratory

of Biochemistry, Department of Chemistry, Universitas Riau. Before conducting any antimicrobial tests, the strains were sub-cultured on fresh agar plates for 24 h.

Minimum inhibitory concentration and minimum bactericidal concentration evaluation

The method described by Army *et al.* was used to calculate the minimum inhibitory concentration (MIC) and minimum bactericidal concentration (MBC) values of the compounds (16). The MIC test was conducted in a 96-well microtiter plate with standard broth microdilution methods, whereas the MBC test was conducted on Mueller Hinton agar (MHA) plates. Both tests were performed using conventional broth microdilution techniques. Before being used, the bacterial inocula was prepared to contain 10^6 colony-forming units (CFU) per mL of solution. After adding 100 µL of a stock solution of extracts with a final concentration of 250 µg/mL for the MIC test, the solution was diluted by a factor of two using bacterial inocula in 100 µL of Muelle-Hinton broth. This was achieved by starting in column 12 and working one column down to column 3. In the microtiter plate column 12 contained the most concentrated extracts, while column 3 contained the least concentrated extracts. Column 1 served as the negative control, consisting only of the medium, whereas column 2 comprised both the medium and the bacterial inoculum. After 24 h of incubation at 37 ℃, the plate was examined to determine whether the density of each well had changed. The MIC was determined by testing antibacterial agents at the lowest concentration known to inhibit bacterial growth. This enabled the most precise results possible. The “MBC” refers to the lowest concentration of antibacterial agents capable of eliminating bacteria. It is also known as the "minimal bactericidal threshold." To conduct the MBC test, a suspension was transferred from each well of the microtiter plates to the MHA plate. Twenty-four hours were spent storing the plates in an incubator at 37 ℃. The MBC was calculated using the lowest concentration at which no visible growth was observed on an MHA plate. Chloramphenicol was used as a positive control, and each experiment was conducted in triplicate.

Molecular docking

Chemdraw Professional 15.0 was used to illustrate the molecular structure of ligands (Fig. 1). The 3D structure was then refined using the Molecular Operating Environment (MOE) 2022.0901 software package (Chemical Computing Group) with the MMFF94x force field and 0.0001 gradient. Using all the molecular structures, a *mdb database of ligands was subsequently created.

The protein's molecular structure was downloaded from the Protein Data Bank (PDB; i.e. wwww.rcsb.org). This work employed three protein targets to target specific functions within cells. The first target (PDB ID: 2ZDQ) aimed to attack cell wall structures. The second target (PDB ID: 1HNJ) aimed to decrease protein synthesis. The third target (PDB ID: 3IL7) aimed to reduce the activity of β-ketoacyl-acyl carrier protein synthase III (KAS III). The protein crystal structure was constructed using the software package “Discovery Studio Visualizer” (DSV, Biovia) and MOE 2022.0901. Utilizing the CHARMM27 force field and a root mean square gradient of 0.01 kcal/mol/A, the energy of this protein was minimized. In addition, the minimization of H atoms, alpha carbon atoms, and backbone atoms was performed with the aid of MOE 2022.0901 (17). This protein was finally saved in PDB format, allowing it to be utilized as a receptor. Before molecular docking, the protein's site-finder must be identified. The active site of the protein was recognized using a site finder. The MDB file containing the pre-made ligand structure was then selected as the ligand, and the dock menu was used to set this site to a dummy atom. Subsequently, the configuration is established in a triangular shape; the adjustment is defined as inflexible, and the position is specified as 50 and 10, correspondingly. The potential was initially established using the CHARMM27 force field, with a grid box of radii x, y, and z measuring 67, 86, and 66, respectively. The optimal docking sites (exhibiting the same binding interaction as the positive control) were chosen based on various criteria, such as binding free energy, root mean square deviation (RMSD), and binding factor.

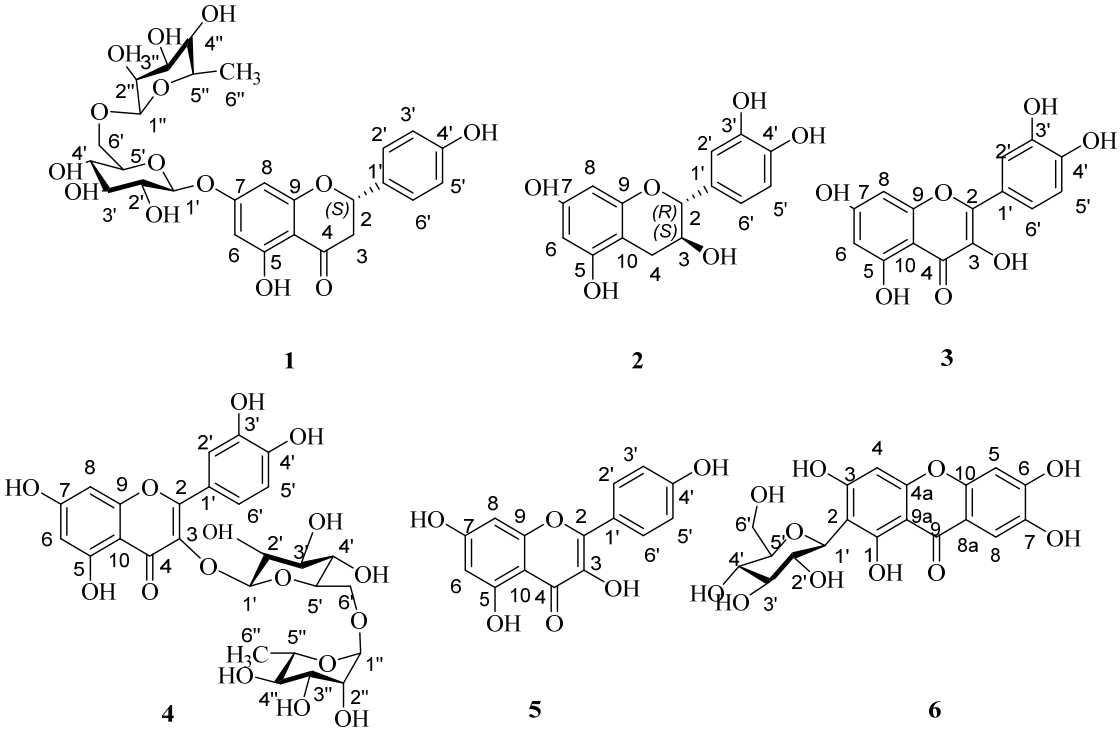

Fig. 1. Molecular structures of isolated compounds 1-6.

Supplementary information

The online version of supplementary material features NMR spectral data of compounds 1-6 laterally with 2D NMR spectral data for these compounds. This supplementary information is accessible at: https://my.unri.ac.id/supplementaryfile.

RESULTS

In this study, the extraction process of *P. longifolia* was undertaken with the liquid-liquid fractionation of the crude methanol extract to produce hexane, dichloromethane, ethyl acetate, and residual fractions. As mentioned in our previous report, the fractions were evaluated for their antibacterial activity, and the results indicated that the ethyl acetate fraction exhibited intermediate antibacterial activity (14). Therefore, this fraction was picked for purification to obtain secondary metabolites using a bioassay-guided approach followed by successive chromatographic works. Vacuum liquid chromatography (VLC) on the fraction afforded sub-fractions that were grouped based on the analysis profile of TLC. Sub-fraction 5 was then purified further using conventional column chromatography, yielding six isolated compounds whose purity was determined using TLC, reverse-phase high-performance chromatography (RP-HPLC), and melting point.

The compounds were employed in molecular structural elucidation through spectrometric and spectroscopic analysis, and their spectral data (NMR and MS) were compared to those reported in the literature, yielding naringin (compound 1) (18), catechin (compound 2) (19), quercetin (compound 3) (20), rutin (compound 4) (21), kaempferol (compound 5) (21), and mangiferin (compound 6) (22) (Fig. 1).

Naringin (1), a white amorphous powder (MeOH); mp 156-158 °C; UV (MeOH) λ_{max} (log ε) 216 (4.15), 237 (3.72), 334 (3.31) nm; IR (KBr) ν_{max} 3350, 2917, 1297, 1096, 1042, 825 cm^{-1}; 1H NMR (DMSO-d6, 500 MHz) δ 7.32 (2H, d, J = 8.5 Hz, H-2'/6'), 6.79 (2H, d, J = 8.5 Hz, H-3'/5'), 6.10 (1H, d, J = 2.5 Hz, H-8), 6.07 (1H, d, J = 2.5 Hz, H-6), 5.51 (1H, dd, J = 2.5 Hz; J = 12 Hz, H-2), 5.11 (H1, d, J = 7.0 Hz, H-1''), 5.08 (H1, s, H-1'''), 3.80 (1H, dd, J = 8.4, 8.0 Hz, H-6a''), 3.62 (1H, dd, J = 8.4 Hz, 8.0 Hz, H-2'''), 3.51 (1H, dd, J = 8.4 Hz, 8.0 Hz,

H-3'"), 3.44 (1H, dd, J = 8.4 Hz, 8.0 Hz, H-5'"), 3.43-3.41 (1H, m, H-2"), 3.40 (1H, t, J = 8.0 Hz, H-3"), 3.37 (1H, dd, J = 8.4 Hz, 8.0 Hz, H-6b"), 3.32-3.33 (1H, m, H-5"), 3.27 (1H, dd, J = 8.4 Hz, 8.0 Hz, H-4'"), 3.24 (1H, dd, J = 8.4 Hz, 8.0 Hz, H-4"), 1.11 (3H, s, H-6'"; 13C NMR (DMSO-d6, 125 MHz) δ 197.7 (C, CO ketone), 165.3 (C, C-7), 163.4 (C, C-5), 163.2 (C, C-9), 158.3 (C, C-4'), 129.1 (C, C-1'), 128.9 (CH, C-2'/6'), 115.7 (CH, C-3'/5'), 103.7 (C, C-10), 100.8 (CH, C-1"), 97.8 (CH, C-1'"), 96.7 (CH, C-6), 95.6 (CH, C-8), 79.08 (CH, C-2), 77.6 (CH, C-3"), 77.4 (CH, C-5"), 76.5 (CH, C-2"), 72.3 (CH, C-3'"), 70.9 (CH, C-2'"), 70.8 (CH, C-3'"), 70.03 (CH, C-4"), 68.0 (CH, C-5'"), 60.89 (CH2, C-6"), 42.6 (CH2, C-3), 18.5 (CH3, C-6'").

Catechin (2), a white amorphous powder (MeOH); mp 136-138 °C; UV (MeOH) λ_{max} (log ε) 236 (3.25), 244 (4.52), 281 (3.41) nm; IR (KBr) ν_{max} 3361, 2937 ,1625, 1523, 1147 cm^{-1}; 1H NMR (DMSO-d6, 500 MHz) δ 9.17 (1H, s, 5-OH), 8.92 (1H, s, 7-OH), 6.71 (1H, d, J = 2.0 Hz, H-2'), 6.68 (1H, d, J = 8.1 Hz, H-5'), 6.58 (1H, dd, J = 8.1 Hz,; J = 2.0 Hz, H-6'), 5.88 (1H, d, J = 2.3 Hz, H-8), 5.68 (1H, d, J = 2.3 Hz, H-6), 4.86 (1H, s, H-3a), 4.47 (1H, d, J = 7.4 H, H-2), 3.81 (1H, dd, J = 13.8; 7.1 Hz, H-3b), 2.65 (1H, dd, J = 16.0; 5.3 Hz, H-4a), 2.34 (dd, J = 16.0, 8.0 Hz, H-4b); 13C NMR (DMSO-d6, 125 MHz) δ 156.9 (C, C-5), 156.6 (C, C-7), 155.8 (C, C7), 145.3 (C, C-3'), 145.5 (C, C-4'), 131.0 (C, C-1'), 118.8 (CH, C-6'), 115.5 (CH, C-5'), 114.9 (CH, C-2'), 99.5 (C, C-9), 95.5 (C, C-8), 94.3 (C, C-6), 81.4 (CH, C-2), 66.7 (CH2, C-3), 28.3 (CH2, C-4).

Quercetin (3), a light yellow amorphous powder (MeOH); mp 224-226 °C; UV (MeOH) λ_{max} (log ε) 256 (4.25), 370 (2.41) nm; IR (KBr) ν_{max} 3007, 2827, 1514, 1170 cm^{-1}; 1H NMR (DMSO-d6, 500 MHz) δ 12.4 (1H, s, 5-OH), 9.29 (1H, s, 3-OH), 7.53 (1H, d, J = 2.0 Hz, H-2'), 7.53 (1H, dd, J = 8.1 Hz,; J = 2.0 Hz, H-6'), 6.83 (1H, d, J = 8.1 Hz, H-5'), 6.39 (1H, d, J = 2.3 Hz, H-8), 6.17 (1H, d, J = 2.3 Hz, H-6); 13C NMR (DMSO-d6, 125 MHz) δ 176.3 (C carbonyl, C-4), 164.3 (C, C-7), 161.2 (C, C-5), 156.6 (C, C-9), 148.2 (C, C-4'), 145.5 (C, C-3'), 147.3 (C, C-2), 122.4 (C, C-1'), 120.4 (CH, C-6'), 116.1 (CH, C-5'), 115.5 (CH, C-2'), 103.46 (C, C-10), 93.8 (C, C-8), 98.6 (C, C-6).

Rutin (4), a yellow amorphous powder (MeOH); mp 240-242 °C; UV (MeOH) λ_{max} (log ε) 258 (5.22), 358 (3.71) nm; IR (KBr) ν_{max} 3070, 1504, 806 cm^{-1}; 1H NMR (DMSO-d6, 500 MHz) δ 1H NMR (DMSO-d6, 500 MHz) δ 12.4 (1H, s, 5-OH), 9.29 (1H, s, 3-OH), 7.53 (1H, d, J = 2.0 Hz, H-2'), 7.53 (1H, dd, J = 8.1 Hz; J = 2.0 Hz, H-6'), 6.83 (1H, d, J = 8.1 Hz, H-5'), 6.39 (1H, d, J = 2.3 Hz, H-8), 6.17 (1H, d, J = 2.3 Hz, H-6), 5.11 (H1, d, J = 7.0 Hz, H-1"), 5.08 (H1, s, H-1'"), 3.80 (1H, dd, J = 8.4, 8.0 Hz, H-6a"), 3.62 (1H, dd, J = 8.4 Hz, 8.0 Hz, H-2'"), 3.51 (1H, dd, J = 8.4 Hz, 8.0 Hz, H-3'"), 3.44 (1H, dd, J = 8.4 Hz, 8.0 Hz, H-5'"), 3.43-3.41 (1H, m, H-2"), 3.40 (1H, t, J = 8.0 Hz, H-3"), 3.37 (1H, dd, J = 8.4 Hz, 8.0 Hz, H-6b"), 3.32-3.33 (1H, m, H-5"), 3.27 (1H, dd, J = 8.4 Hz, 8.0 Hz, H-4'"), 3.24 (1H, dd, J = 8.4 Hz, 8.0 Hz, H-4"), 1.11 (3H, s, H-6'"; 13C NMR (DMSO-d6, 125 MHz) δ 197.7 (C, CO ketone), 165.3 (C, C-7), 163.4 (C, C-5), 163.2 (C, C-9), 158.3 (C, C-4'), 129.1 (C, C-1'), 128.9 (CH, C-2'/6'), 115.7 (CH, C-3'/5'), 103.7 (C, C-10), 100.8 (CH, C-1"), 97.8 (CH, C-1'"), 96.7 (CH, C-6), 95.6 (CH, C-8), 79.08 (CH, C-2), 77.6 (CH, C-3"), 77.4 (CH, C-5"), 76.5 (CH, C-2"), 72.3 (CH, C-3'"), 70.9 (CH, C-2'"), 70.8 (CH, C-3'"), 70.03 (CH, C-4"), 68.0 (CH, C-5'"), 60.89 (CH2, C-6"), 42.6 (CH2, C-3), 18.5 (CH3, C-6'").

Kaempferol (5), a light yellow amorphous powder (MeOH); mp 276 -278 °C; UV (MeOH) λ_{max} (log ε) 266 (4.55), 368 (2.61) nm; IR (KBr) ν_{max} 3311, 1660, 1506 cm-1; 1H NMR (DMSO-d6, 500 MHz) δ 12.4 (1H, s, 5-OH), 8.03 (2H, d, J = 9.0 Hz, H-3'/5'), 6.91 (2H, d, J = 9.0 Hz, H-2'/6'), 6.39 (1H, d, J = 2.3 Hz, H-8), 6.17 (1H, d, J = 2.3 Hz, H-6); 13C NMR (DMSO-d6, 125 MHz) δ 176.3 (C carbonyl, C-4), 164.3 (C, C-7), 161.2 (C, C-5), 156.6 (C, C-9), 159.6 (C, C-4'), 147.3 (C, C-2), 136.1 (C, C-3), 129.9 (C, C-3'/5'), 122.4 (C, C-1'), 115.9 (CH, C-2'/6'), 103.4 (C, C-10), 93.8 (CH, C-8), 98.6 (CH, C-6).

Mangiferin (6), a white amorphous powder (MeOH); mp 252 -254 °C; UV (MeOH) λ_{max} (log ε) 256 (3.55), 316 (1.61) nm; IR (KBr) ν_{max} 3365, 2937, 1622, 1348 cm^{-1}; 1H NMR (DMSO-d6, 500 MHz) δ 13.7 (1H, s, 1-OH), 7.36 (1H, s, H-8), 6.84 (1H, s, H-5), 6.36 (1H, s, H-4), 4.58 (1H, d, J = 9.8 Hz, H-1'), 4.03 (1H,

t, J = 9.2 Hz, H-4'), 3.68 (1H, d, J = 3.68, H-6'a), 3,37-3.41 (1H, m, H-6'b), 3.07-3.20 (3H, m, H-2',3',5'); 13C NMR (DMSO-d6, 125 MHz) δ 179.5 (C carbonyl, C-9), 164.3 (C, C-3), 162.2 (C, C-1), 156.7 (C, C-4a), 154.8 (C, C-6), 144.2 (C, C-7), 112.1 (C, C-8a), 108.4 (C, C-8), 108,1 (CH, C-2), 103.0 (CH, C-5), 101.7 (C, C-9a), 93.7 (CH, C-4), 82.0 (CH, C-5'), 79.4 (CH, C-3'), 73.5 (CH, C-1'), 71.1 (CH, C-2'), 70.7 (CH, C-4'), 61.9 (CH2, C-6').

Figure 1 shows that compounds 1 and 2 have stereocenters at C-2, and C-2 and C-3, respectively. Therefore, circular dichroism (CD) spectroscopy was employed to determine the precise arrangement of compounds 1 and 2. Figure 2A and B depict the CD spectra of these substances.

Furthermore, the compounds' antibacterial activity was evaluated against *B. subtilis*, *B. cereus*, *S. aureus*, *L. monocytogenes*, and *V. alginolyticus*. The microdilution method was utilized to determine their efficacy which entails diluting the compounds and measuring their MIC and the MBC as shown in Table 1.

Of the evaluated compounds, kaempferol (**5**) exhibited a particularly potent antibacterial activity, with MIC values between 7.8 and 62.5 µg/mL, especially against *B. subtilis* and *S. aureus*. Kaempferol demonstrated significant bactericidal activity, with minimum bactericidal concentration (MBC) values between 15.6 and 125 µg/mL, indicating its potential as a robust antibacterial agent. Furthermore, rutin (**4**) demonstrated notable antibacterial properties, especially against *S. aureus* and *B. cereus*, with MIC values between 15.6 and 250 µg/mL. The MBC values were comparably effective, suggesting that rutin may be a promising antibacterial agent, albeit less potent than kaempferol.

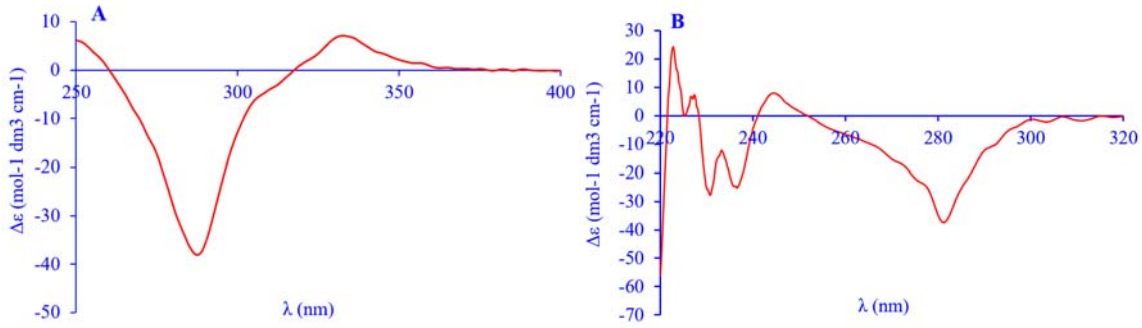

Fig. 2. Circular dichroism spectra of (A) compound 1 and (B) compound 2 (MeOH, 25 °C).

Table 1. Minimum inhibition concentration and minimum bactericidal concentration of compounds 1-6.

Compounds	*B. subtilis* ATCC 9659	*B. cereus* ATCC 10876	*S. aureus* ATCC 6538	*L. monocytogenes* ATCC 7644	*V. alginolyticus* ATCC 17749
			Minimum inhibition concentration (µg/mL)		
1	7.8	62.5	15.6	125	250
2	15.6	62.5	7.8	125	125
3	31.2	62.5	7.8	250	62.5
4	31.2	62.5	15.6	250	62.5
5	7.8	62.5	15.6	31.2	31.2
6	31.2	62.5	15.6	125	125
Chloramphenicol	15.6	7.8	7.8	7.8	7.5
			Minimum bactericidal concentration (µg/mL)		
1	31.2	250	62.5	250	> 250
2	15.6	250	62.5	> 250	> 250
3	125	125	31.2	> 250	250
4	62.5	125	15.6	250	250
5	31.2	125	15.6	125	62.5
6	62.5	125	15.6	250	250
Chloramphenicol	15.6	15.6	31.2	7.8	15.6

Naringin (**1**) and catechin (**2**) exhibited moderate antibacterial efficacy, with MIC values ranging from 7.8 to 250 µg/mL. Both compounds exhibited notable activity against *S. aureus*; however, their effectiveness against *V. alginolyticus* and *L. monocytogenes* was constrained, as indicated by the elevated MIC values for these strains. Moreover, quercetin (**3**) exhibited moderate antibacterial activity, with MIC values comparable to those of catechin and naringin. It demonstrated notable efficacy against B. subtilis, indicating its potential as an antibacterial agent against gram-positive bacteria. Mangiferin (6) demonstrated the least antibacterial efficacy among the isolated compounds, with MIC values between 31.2 and 250 µg/mL. Its diminished efficacy against *V. alginolyticus* and *L. monocytogenes* indicates that it may possess restricted utility as an antibacterial agent.

In comparison to chloramphenicol, the positive control, the isolated compounds typically demonstrated elevated MIC and MBC values. Nonetheless, the findings suggest that certain compounds, notably kaempferol and rutin, exhibit considerable antibacterial efficacy, particularly against gram-positive bacteria.

In addition, as further evidence for the finding, in this study, we reported the results of the *in-silico* study of the antibacterial mechanisms of the compounds. To elucidate ligand interactions with protein binding sites, the compounds were docked as ligands into protein targets to attack cell walls (PDB ID: 2ZDQ) (Table 2) and inhibit protein synthesis (PDB ID: 1HNJ) (Table 3), as well as to reduce the activity of β-ketoacyl-acyl carrier protein synthase III (PDB ID: 3IL7) (Table 4).

Table 2. Docking results for PDB ID 2ZDQ.

Compound	Binding free energy (kcal/mol)	RMSD	H bond	Hydrophobic interaction	Van der Waals Interaction	Others interaction	Binding factor
1	-7.5137	1.5244	Glu 327 Arg 357 Tyr 358	-	Asp 213 Asp 214	Asn 113 Asn 271 Leu 177 Gly 114 Asn 178 Asn 233 Val 232 Val 188 Thr 180 Thr 270 His 267 Phe 230 Gly 324 Gln 266 Pro 354 Asn 211 Ala 328	22
2	-7.6709	1.1238	-	Arg 37 Arg 186	Glu 423	Leu 13 Thr 36 Thr 16 Gly 17 Asn 421 Leu 15 Asn 138 Phe 422 Phe 161 His 183 Leu 416 Pro 72 Gly 12 Gly 73 Ser 71	18

Table 2. Continued

3	-7.6974	1.2342	Asn 421	Arg 37	Glu 423	Gly 12 Phe 422 Asn 138 Leu 13 Thr 16 Pro 72 Gly 73 Ser 71 Ala 414 His 183 Ser 415 Leu 416 Leu 15 Phe 161 Thr 321 Thr 36	19
4	-7.9442	1.8783	Gln 193 Glu 164 Arg 200		Glu 203	Phe 189 Ala 197 Ala 196 Gln 192 Ala 77 Ser 167 Leu 76 Asn 204	21
5	-7.4159	0.8919	Gly 73	Arg 37 Arg 186	Glu 423	Gly 12 Pro 72 Ser 71 Thr 16 Thr 36 Asn 138 Asn 421 Phe 161 Phe 422 Leu 15 His 183 Leu 416 Leu 13	17
6	-7.3611	1.8738	-	Lys 115 Arg 37 Arg 186	-	Ser 159 Asn 421 Phe 422 Asn 138 Leu 15 Thr 16 Gly 14 Gly 17 Ser 71 Thr 36 Gly 73 Pro 72 Leu 416 Ser 415 Phe 161 His 183 Ala 414	21
Chloramphenicol	-8.8972	0.7643	-		Glu 203	Phe 189 Ala 197 Ala 196 Gln 192 Ala 77 Ser 167 Leu 76 Asn 204	

RMSD, Root mean square deviation.

Table 3. Docking results for PDB ID 1HNJ.

Compound	Binding free energy (kcal/mol)	RMSD	H bond	Hydrophobic interaction	Van der Waals interaction	Others interaction	Binding factor
1	-7.0438	1.6502	Tyr 182 Leu 318 Glu 96 Glu 184	Arg 84 Arg 181 Lys 138 Arg 264 Lys 100	-	Pro 101 Gly 99 Thr 319 Val 206 Phe 85 Asn 205	15
2	-6.2362	1.5105	Glu 96 Asp 115 Arg 84	Arg 264	Asp 88 Asp 183 Glu 184	Gly 106 Tyr 102 Asn 156 Ala 108 Ala 317	12
3	-6.3010	1.1178	Gly 106	Arg 84 Lys 100 Arg 264	Glu 96 Glu 184 asp 183	Tyr 102 Pro 101 Leu 118 Val 107 Ala 109 Gly 262 Leu 95 Ala 108	15
4	-8.6516	1.6132	Glu 184 Arg 84 Asp 40 Glu 96	Arg 181 Arg 264 Lys 100	-	Phe 85 Tyr 182 Gly 41 Ser 11 Pro 12 Leu 97 Gly 99 Val 10 Leu 98 Pro 101	17
5	-6.5317	1.8463	Glu 96 Asp 183	Arg 137 Arg 84 Arg 264 Lys 100	Asp 88 Glu 184	Ala 108 Tyr 102 Ala 317 Pro 101 Gly 104 Val 107 Gly 262 Asn 156 Val 206 Gly 106 Phe 85	19
6	-6.3807	1.9164	Pro 67		Glu 72	Ser 70 Trp 71 Leu 69 Pro 66 Trp 71 Pro 64 His 63 Pro 67 Pro 66 Leu 69 Pro 68 Pro 68	14
Chloramphenicol	-8.9872	0.6132	Glu 184 Arg 84 Asp 40 Glu 96	Arg 181 Arg 264 Lys 100	-	Phe 85 Tyr 182 Gly 41 Ser 11 Pro 12 Leu 97 Gly 99 Val 10 Leu 98 Pro 101	

RMSD, Root mean square deviation.

Table 4. Docking results of compound **4** for PDB ID 3IL7.

Compound	Binding free energy (kcal/mol)	RMSD	H bond	Hydrophobic interaction	Van der Waals interaction	Others interaction	Binding factor
4	-8.2498	1.3782	His 193 Glu 164 Arg 200	-	Glu 203	Phe 189 Ala 197 Ala 196 Gln 192 Ala 77 Ser 167 Leu 76 Asn 204	22
Chloramphenicol	-9.2791	0.9820	His193	-	Glu 203	Phe 189 Ala 197 Ala 196 Gln 192 Ala 77 Ser 167 Leu 76 Asn 204	-

RMSD, Root mean square deviation.

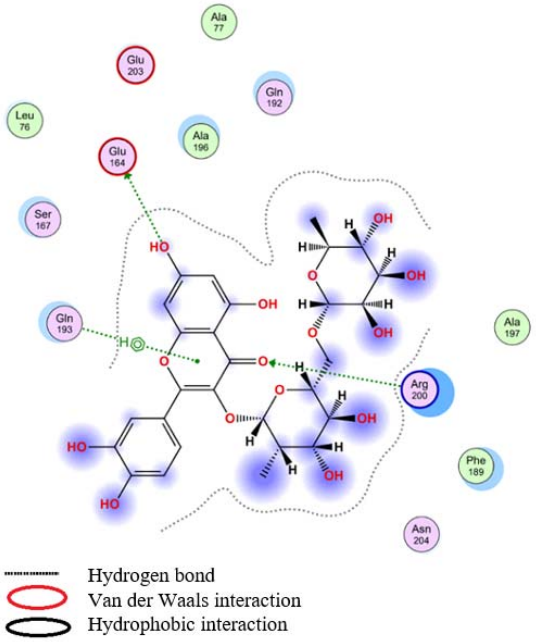

Fig. 3. Spatial arrangement of compound 4 with protein target (PDB ID; 2ZDQ).

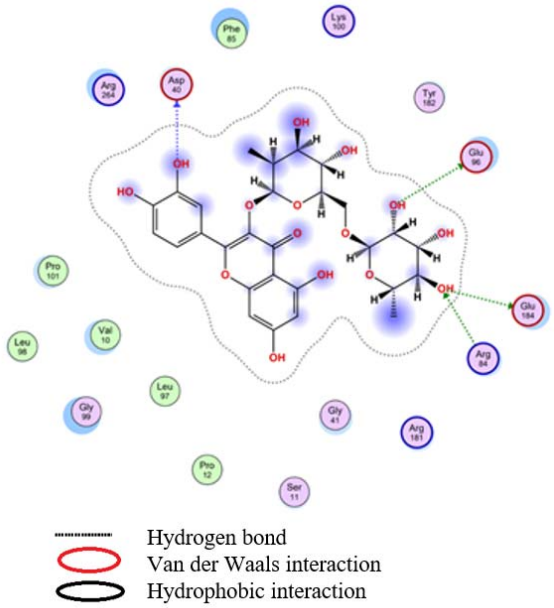

Fig. 4. Spatial arrangement of compound 4 with protein target PDB 1HNJ.

Figures 3-6 illustrate the spatial configuration of compound **4** with the three distinct protein targets, offering a visual representation of the docking outcomes. Figure 3 depicts the interaction of compound 4 with D-alanine-D-alanine ligase (PDB ID: 2ZDQ), whereas Fig. 4 presents its interaction with the ribosomal protein target (PDB ID: 1HNJ). Figure 5 illustrates the interaction of compound 4 with β-ketoacyl-acyl carrier protein synthase III (PDB ID: 3IL7), while Fig. 6 elucidates the inhibitory mechanism of flavonoids as β-ketoacyl-acyl carrier protein synthase III antagonists. These data underscore the essential hydrogen bonding and hydrophobic interactions that enhance the antibacterial properties of the compounds.

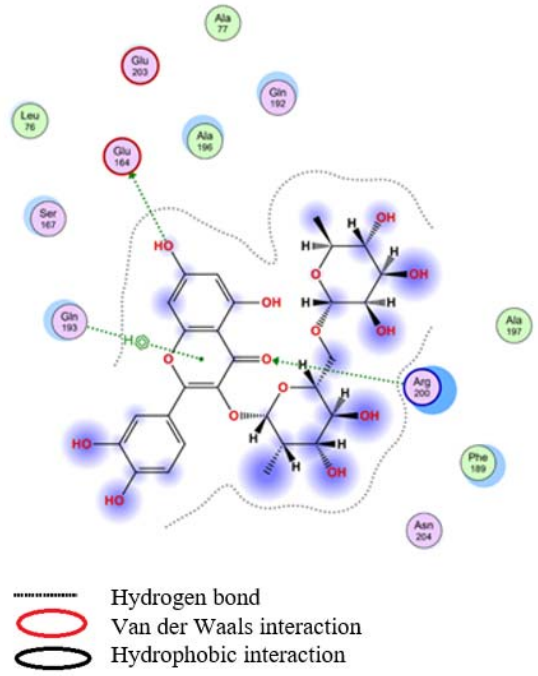

Fig. 5. Spatial arrangement of compound 4 with protein target PDB 3IL7.

Rutin (**4**) exhibited the highest binding affinity, with a binding free energy of -7.9442 kcal/mol for PDB ID: 2ZDQ and -8.6516 kcal/mol for PDB ID: 1HNJ. Rutin established numerous hydrogen bonds with residues critical for bacterial cell wall and protein synthesis, including Gln193, Glu164, and Arg200. These robust interactions indicate that rutin effectively impedes essential bacterial processes, corroborating its documented antibacterial efficacy. Kaempferol (**5**) exhibited robust binding, especially towards PDB ID: 3IL7, with a binding free energy of -8.2498 kcal/mol. kaempferol's interaction with His193, Glu164, and Arg200 indicates its inhibition of fatty acid biosynthesis, essential for bacterial membrane formation, thereby elucidating its potent antibacterial efficacy against gram-positive bacteria.

Naringin (**1**) and catechin (**2**) exhibited moderate binding affinities, with binding free energies of -7.6709 kcal/mol and -7.5137 kcal/mol, respectively, for PDB ID: 2ZDQ. These compounds established fewer hydrogen bonds than rutin and kaempferol, resulting in less effective inhibition of bacterial targets, which aligns with their comparatively elevated MIC values. Quercetin (**3**) exhibited moderate binding interactions with both PDB ID: 2ZDQ and PDB ID: 1HNJ, corroborating its noted antibacterial efficacy, especially against *S. aureus*. Mangiferin (**6**) demonstrated the weakest binding interactions among all protein targets, aligning with its diminished antibacterial activity in vitro. The docking results correspond with the in vitro findings, demonstrating that rutin and kaempferol possess the most significant potential for antibacterial activity via their interactions with bacterial enzymes. These compounds signify promising prospects for additional advancement as antibacterial agents.

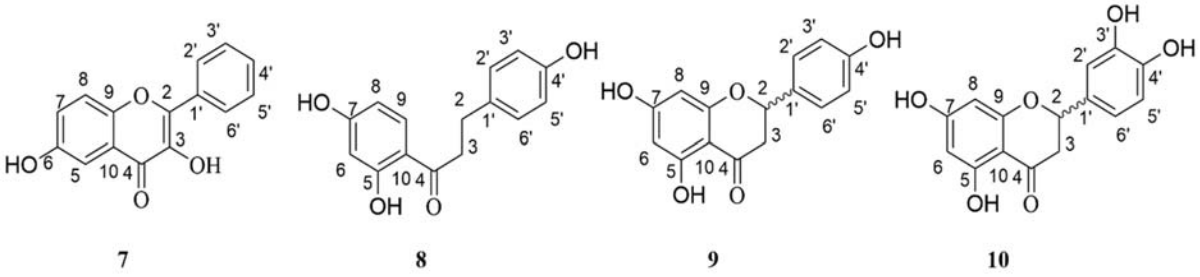

Fig. 6. Flavonoids as β-ketoacyl-acyl protein synthase III inhibitors.

DISCUSSION

A prior investigation by Khodijah *et al.* demonstrated that the ethyl acetate extract derived from this particular species (*P. longifolia*) displayed superior antibacterial efficacy compared to the extracts obtained from the species (14). Hence, the current study purified and isolated the secondary metabolites from the ethyl acetate extract, and employed a bioassay-guided technique. Six phenolic compounds were obtained from this investigation utilizing spectroscopic methods. Compounds 1 and 2, out of the six compounds, had stereocenters, which required additional study using CD spectroscopy. The results showed that the stereo-orientation of these compounds was 2S (compound 1), and 2R and 3S (compound 2). The study also documented the antimicrobial efficacy of all six compounds. The antibacterial efficacy was assessed by determining MIC and MBC. The results varied significantly when compared to the positive control, chloramphenicol. The significance of the exploration for natural compounds with antibacterial properties is emphasized, along with the limited documentation of the antibacterial activity of this specific species, especially the compounds found within it that demonstrate such activity.

Compound 1, identified as naringin, is classified as a flavanone due to its absence of a double bond between carbon atoms 2 and 3 and the occurrence of a stereocenter at carbon atom 2. On the other hand, compound 2, catechin, possesses two stereocenters at carbon atoms 2 and 3. The absolute configurations of the compounds were determined using CD spectroscopy, as shown in Fig. 2A and B. The CD spectra of naringin exhibited cotton effects at 287 and 332 nm, with corresponding Δε values of -38.09 and +7.09, respectively. The data, in addition to the UV absorption patterns, verified that naringin is (2S)-naringin. This confirms the α-direction of its C2-phenyl group and establishes a 2S configuration. The presence of a substantial J2,3 coupling constant of 17 Hz further supports the equatorial orientation of the C-2-aryl group. However, catechin's structure is characterized by a chroman chromophore, which causes a chiral distortion in the achiral benzene A-ring. This is supported by the observation of cotton effects at 240 nm (Δε: +8.04) and 280 nm (Δε: -37.47), indicating a 2R,3S-trans configuration (23-26). The NMR data, which includes a J2,3 coupling constant of 7.4 Hz and a negative cotton effect at 280 nm, supports the 2R configuration. This confirms the unique stereochemical characteristics of these two naturally occurring compounds.

P. longifolia is an epiphytic fern species in the *Pyrrosia* genus known for its medicinal properties in Indonesia and the Pacific Countries. This species has traditionally been used to relieve labor-related pains, but despite its widespread use, the phytochemical and biological activities of the species are still being studied. Even though we reported six known compounds in our study, we also described the absolute configurations of compounds **1** and **2**. These compounds were reported for the first time within this species, and compound **1** was reported for the first time in both this species and its genus. The absolute configuration of **1** is comparable to that of its parent structure, naringenin, which was isolated from *P. petiolosa*; however, the report has not provided any explanation for its configuration in any detail (3). Moreover, compounds 2-6 were found in various species of *Pyrrosia*, such as in *P. davidii, P. petiolosa, P. sheareri,* and *P. calvata* (6,8,9,27).

In addition, the antibacterial activity of the compounds was evaluated against *B. subtilis, B. cereus, S. aureus, L. monocytogenes,* and *V. alginolyticus*. A serial dilution method was employed to accurately evaluate the compounds' efficacy by calculating the MIC by which the effective antibacterial concentrations against each bacterial strain tested were determined (28).

The MICs of compounds 1-6 against the tested bacteria are detailed in Table 1. The MIC values ranging from 7.8 to 250 µg/mL were observed. Notably, each compound displayed high antibacterial activity against *B. subtilis*, outperforming all other tested bacteria. Compound 5 had MIC values ranging from 7.8 to 62.5 µg/mL against the tested pathogens. Moreover, the MIC value of compound 2 was comparable to that of chloramphenicol. Despite

this, it is worth noting that the MIC values of the compounds were higher than chloramphenicol (Table 1).

The MBC, also known as the minimum lethal concentration, of the compounds as potential antimicrobial agents was determined. MBC is the minimum concentration of an antimicrobial agent required to kill 99.9% of the initial inoculum after 24 h of incubation (29). By applying the compounds to this test, we could determine their effectiveness against the specified microorganisms. The MBC test is a key indicator of the compounds' efficacy as antimicrobial agents by measuring their capacity to eradicate bacterial growth, completely. In conjunction with the MIC values determined earlier, these findings afford a comprehensive understanding of the compound's ability to inhibit and eradicate bacterial growth, indicating their potential as potent antimicrobial agents. The MBC values were greater than the MIC values, indicating that the antibacterial activity of the compounds was concentration-dependent. To subdue the bacterial cells, a higher concentration of the compound was required than just to inhibit their growth. Surprisingly, our findings showed that the MBC value of compound 2 was the same as its MIC, and it is comparable to chloramphenicol in this regard (Table 1). Overall, the inhibitory activity of the tested compounds could be considered bactericidal, as the ratio between MBC and MIC was determined to be less than 4.

Resazurin was added as an additional color indicator in this antibacterial test., Addition of resazurin to the testing procedure permits qualitative (visual) prediction of antibacterial activity *via* color changes. Resazurin is a blue dye internalized by cells and metabolically reduces to resorufin, a highly fluorescent pink compound, that is freely released from the cells. The intracellular enzyme diaphorase catalyzes the conversion of resazurin to irreversible resorufin, resulting in a strong fluorescent signal that can be measured using a spectrophotometer to assess the cell population's comprehensive metabolic activity (30,31).

Compounds 1 through 5 have been identified as flavonoids, which have been reported to possess antibacterial properties. Flavonoids exert antibacterial effects *via* multiple mechanisms, including inhibition of nucleic acid synthesis, cytoplasmic membrane function, energy metabolism, attachment and biofilm formation, inhibition of porins, membrane permeability modification, and attenuation of pathogenicity. Although the antibacterial potential of flavonoids is promising for combating antibiotic-resistant microorganisms, the vast majority of studies have focused on *in vitro* testing, with limited research into their *in vivo* activity (32). Studies on the structure-activity relationship and mechanism of flavonoids have demonstrated that the presence of hydroxyl groups at certain places increases the efficacy of flavones, flavanones, and chalcones. Notably, substitutions like 5,7-dihydroxylation and hydroxylation at the 2' or 4' positions are linked to heightened activity. In contrast, the methylation of hydroxyl groups tends to reduce their bioactivity. The lipophilicity of the A ring significantly influences the chalcone's bioactivity. Hydrophobic substituents, such as prenyl groups and alkyl chains, are discovered to augment their bioactivity (33).

The moderate efficacy of naringin (1), catechin (2), and quercetin (3) indicates that although these compounds can inhibit bacterial growth, their physical properties constrain their potency relative to kaempferol and rutin. The stereocenters in naringin and catechin, along with the substitution patterns of hydroxyl groups in quercetin, may diminish their binding efficacy with bacterial enzymes, as indicated by their elevated MIC values. Mangiferin (6), characterised by a reduced number of hydroxyl groups and a more rigid conformation, demonstrated the least antibacterial activity, suggesting that these structural attributes may diminish its capacity to interact effectively with bacterial targets.

As further evidence for the finding, we reported in this study, the results of the *in-silico* study of the antibacterial mechanisms of the compounds. To elucidate ligand interactions with protein binding sites, the compounds were docked as ligands into protein targets to attack cell walls (PDB ID: 2ZDQ) and inhibit protein synthesis (PDB ID: 1HNJ). Table 2 shows the

docking results, which show that these compounds have a strong affinity for the receptor's active and allosteric sites. The best complex ligand-protein poses were chosen based on the lowest binding free energy value with the lowest RMSD value. Based on the docking results, compound 4 is predicted to be a good inhibitor of cell wall attack. Compound 4, the estimated active compound, has the lowest binding free energy of -7.9442 kcal/mol and interacts with Gln193, Gln164, and Arg200 *via* hydrogen bonds. This compound had a van der Waals interaction with Glu203. Because of the presence of a hydroxy group, compound 4 has a lower binding free energy than the other compounds (17).

Intriguingly, one antibacterial interacts with three of the four amino acid residues in the cocrystal ligand when it is used to inhibit the formation of cell walls (enzyme D-alanine: D-alanine ligase, PDB ID 2ZDQ). This demonstrates that the interactions between the antibacterial and the natural substrate of the 2ZDQ receptor, ATP in this case, are identical. Compound 4 interacted with three alanine amino acid residues, namely Ala77, Ala196, and Ala197. The 2ZDQ receptor is a ligase enzyme that requires ATP as a phosphate source. Compound 4, which lacks a phosphate group and binds ATP to the active side of the receptor, inhibits the microbial cell wall catalysis process. It can directly eliminate microorganisms (34,35). Compound 4 can likely be employed as an antibacterial agent that attacks cell wall synthesis.

The docking results of compound 4 were also superior to those of other compounds. It showed a binding free energy of -8.6516 kcal/mol and a binding factor of 17. Binding free energy is the most important parameter in docking, and the binding factor; is defined as the similarity between amino acid residues and the native ligand. Compound 4 has the lowest binding free energy, suggesting that it requires the least quantity of energy to inhibit protein synthesis. They need more energy than other compounds to inhibit protein synthesis. Significant differences between the cell wall architectures of gram-negative and gram-positive bacteria may account for the inhibitory effects. The cell walls of gram-negative bacteria consist of an additional outer membrane and a thin peptidoglycan layer (7-8 nm). Gram-positive bacteria lack an outer membrane and have a thick peptidoglycan layer (20-80 nm) outside the cell wall (36). A polymer resembling a mesh made of sugars and amino acids is called peptidoglycan. Antibacterial substances like antibiotics, poisons, chemicals, and degradative enzymes are all prevented from harming the microorganism by the peptidoglycan layer.

Compound 4 formed four hydrogen bonds with the amino acid residues Arg184, Glu84, Asp40, and Glu96 based on the docking results. Furthermore, this compound interacts with the amino acids Arg181, Arg264, and Lys100 *via* a hydrophobic interaction. Based on this interaction, hydrophobic fragments may play an important role in binding with the molecule to inhibit protein synthesis. Furthermore, the attack of bare peptidoglycan in the cell wall may be responsible for the inhibitory effectiveness of the chemicals produced against bacterial growth. As a result, these substances were assumed to have beneficial biological effects. Figure 4 depicts the spatial arrangement of compound 4.

Furthermore, in this *in-silico* study, isolated compounds were tested for their potential as antibacterial agents using KAS III. Based on the *in-silico* results against the aforementioned proteins, compound 4 emerged as the most promising candidate. Consequently, molecular docking of compound 4 with KAS III (PDB ID 3IL7) was carried out. The reason for selecting this protein is that KAS III is a functioning enzyme in fatty acid synthase. Because it stimulates fatty acid synthesis, which is essential in bacterial fatty acid biosynthesis, its inhibitors can serve as potent antibiotics with broad-spectrum activity. Hence, KAS III presents an attractive target for the design of novel antimicrobial drugs (37). According to Table 4, compound 4 showed a binding free energy of -8.2498 kcal/mol when it was docked in KAS III. Additionally, it formed hydrogen bonding in contact with His193, Glu164, and Arg200. The amino acids have a significant resemblance to the docking outcomes of compound 4 with protein 2ZDQ, which specifically interacts with the bacterial cell

wall. Given this resemblance, it is evident that compound 4 can serve as an antibacterial agent. Moreover, the KAS III sequences with antibacterial properties and 2ZDQ exhibit a resemblance of more than 55%, but the similarity of their active site residues surpasses 80%. The significant resemblance in the active areas provides more evidence for the potential of compound 4 to be a powerful antibacterial agent against targets that share similar structural characteristics with KAS III and 2ZDQ.

Figure 5 demonstrates that the inhibitory mechanism of compound 4 against KAS III is achieved by establishing certain hydrogen bonds. Specifically, the 7-OH hydroxyl groups of compound 4 interact with Glu164, while its carbonyl functional group interacts with Arg200. The findings of this computational analysis are consistent with the earlier investigation conducted by Lee *et al*. which showed that 3,6-dihydroxyflavone (7) and phloretin (8) (Fig. 6) establish hydrogen bonds between their hydroxyl groups and the backbone carbonyl oxygen of Phe304 and Gly209, respectively (37). In addition, Lee *et al.* conducted molecular docking experiments to examine the interaction between naringenin (9) and eriodictyol (10) with KAS III (Fig. 6). The results showed that the inhibitory mechanism includes the formation of hydrogen bonds between the hydroxyl groups of the flavonoids and the backbone carbonyl oxygen of certain amino acids in KAS III. More precisely, the hydroxyl groups at positions 4' and 7 of these flavonoids form hydrogen bonds with the carbonyl groups of Phe298 and Ser152 in the backbone (38). Hence, this interaction plays a crucial role in the antimicrobial effectiveness of flavonoids, highlighting their potential as building blocks for the creation of novel antimicrobial substances that specifically inhibit fatty acid production in bacteria.

CONCLUSION

The phytochemical study conducted on the fern *P. longifolia* yielded six compounds using a bioassay-guided approach. Additionally, the absolute configurations of compounds 1 and 2 were reported for the first time in this species. The antibacterial activities of the compounds showed a variety of different activities towards the bacteria that were tested. According to this finding, both *B. subtilis* and *S. aureus* were susceptible to the compounds. In addition, these compounds have a strong affinity for the active and allosteric sites of the receptor, allowing them to attack cell walls and inhibit protein synthesis. Compound 4 was predicted to be a good inhibitor of cell wall attack, and the other compounds had the same properties.

Acknowledgments

We gratefully acknowledge support from the Ministry of Education, Culture, Research and Technology of the Republic of Indonesia and the Center of Research and Community Development, University of Riau, and the research was funded by the University of Riau through Grant No. 1635/UN19.5.1.3/PT.01.03/2022.

Conflict of interest statement

The authors declared no conflict of interest in this study.

Authors' contribution

R. Hendra conceptualized the projects, revised the manuscript, and provided financial support; R. Khodijah isolated the compounds and assessed their antibacterial activities; H.Y. Teruna wrote the manuscript and elucidated the structure; and N. Frimayanti carried out the *in-silico* study and revised the manuscript. All authors read and approved the finalized article.

REFERENCES

1. Tsutsumi C, Praptosuwiryo TN, Kato M. A preliminary study on mild hemiparasitic epiphytic fern *Pyrrosia piloselloides* (Polypodiaceae). Bull Natl Mus Nat Sci, Ser B. 2018;44(3):121-125. DOI: 10.31557/APJCP.2019.20.1.185.
2. Committee CNP. Pharmacopoeia Chinensis Ren ZH, He MG, Dian GY, editors. China: Chemistry Engineering Publishers, Beijing; 2000.
3. Yang C, Shi JG, Mo SY, Yang YC. Chemical constituents of *Pyrrosia petiolosa*. J Asian Nat Prod Res. 2003;5(2):143-150. DOI: 10.1080/1028602031000066843.
4. Cheng D, Zhang Y, Gao D, Zhang H. Antibacterial and anti-inflammatory activities of extract and

fractions from *Pyrrosia petiolosa* (Christ et Bar.) Ching. J Ethnopharmacol. 2014;155(2):1300-1305. DOI: 10.1016/j.jep.2014.07.029.
5. Brownsey P, Shepherd L, de Lange P, Perrie L. *Pyrrosia serpens* (G. Forst.) Ching a new record for the fern flora of the Kermadec Islands. N Z J Bot. 2021;59(2):229-243. DOI: 10.1080/0028825X.2020.1796716.
6. Lang TQ, Zhang Y, Chen F, Luo GY, Yang WD. Characterization of chemical components with diuretic potential from *Pyrrosia petiolosa*. J Asian Nat Prod Res. 2021;23(8):764-771. DOI: 10.1080/10286020.2020.1786065.
7. Akhmadjon S, Hong SH, Lee EH, Park HJ, Cho YJ. Biological activities of extracts from Tongue fern (*Pyrrosia lingua*). J Appl Biol Chem. 2020; 63(3):181-188. DOI: 10.3839/JABC.2020.025.
8. He K, Fan LL, Wu TT, Du J. A new xanthone glycoside from *Pyrrosia sheareri*. Nat Prod Res. 2019;33(20):2982-2987. DOI: 10.1080/14786419.2018.1514398.
9. Chen YJ, Xie GY, Xu GK, Dai YQ, Shi L, Qin MJ. Chemical constituents of *Pyrrosia calvata*. Nat Prod Commun. 2015;10(7):1191-1193. PMID: 26411008.
10. Wang N, Wang JH, Li X, Ling JH, Li N. Flavonoids from *Pyrrosia petiolosa* (Christ) Ching: Note. J Asian Nat Prod Res. 2006;8(8):753-756. DOI: 10.1080/10286020500246550.
11. Austin DE. Plant resources of South-East Asia No 15(2): Ferns and Fern Allies. Econ Bot. 2003;57(3):432,170-174. DOI: 10.1663/0013-0001(2003)057[0432:BREDFA]2.0.CO;2.
12. Nugraha AS, Triatmoko B, Wangchuk P, Keller PA. Vascular epiphytic medicinal plants as sources of therapeutic agents: their ethnopharmacological uses, chemical composition, and biological activities. Biomolecules. 2020;10(2):181,1-66. DOI: 10.3390/biom10020181.
13. Khodijah R, Teruna HY, Hendra R. Antioxidant and α-glucosidase inhibition of *Pyrrosia longifolia* extracts. J Pharm Educ. 2022;22(2):16-19. DOI: 10.46542/pe.2022.222.1619.
14. Khodijah R, Haryani Y, Teruna HY, Hendra R. Antibacterial properties of *Pyrrosia longifolia* extracts. J Pharm Educ. 2023;23(2):168-173. DOI: 10.46542/pe.2023.232.168173.
15. Baig MH, Ahmad K, Rabbani G, Danishuddin M, Choi I. Computer aided drug design and its application to the development of potential drugs for neurodegenerative disorders. Current neuropharmacology. 2018;16(6):740-748. DOI: 10.2174/1570159X15666171016163510.
16. Army MK, Khodijah R, Haryani Y, Teruna HY, Hendra R. Antibacterial *in vitro* screening of *Helminthostachys zeylanica* (L.) Hook. root extracts. J Pharm Pharmacogn Res. 2023;11(2):291-296. DOI: 10.56499/jppres22.1540_11.2.291.
17. Frimayanti N, Chee CF, Zain SM, Rahman NA. Design of new competitive dengue Ns2b/Ns3 protease inhibitors-a computational approach. Int J Mol Sci. 2011;12(2):1089-1100. DOI: https://doi.org/10.3390/ijms12021089.
18. Piao XL, Wu Q, Han S, Kim HY, Lee SH. Simultaneous determination of flavanone glycosides in the fruit of *Citrus paradisi* and *C. grandis* by HPLC-PDA. Nat Prod Sci. 2011;17(4):337-341. DOI: 10.20307/nps.2016.22.4.231.
19. Supriatno S, Hidayat AT, Farabi K, Abdullah FF, Nurlelasari N, Herlina T, *et al*. Flavanoids from the stembark of *Chisocheton pentandrus* (*Meliaceae*). J Kimia VALENSI. 2017;3(2):123-127. DOI: 10.15408/jkv.v0i0.6077.
20. Hendra R, Keller PA. Flowers in Australia: phytochemical studies on the *Illawarra flame* tree and Alstonville. Aust J Chem. 2016;69:925-927. DOI: 10.1071/CH16058.
21. Hendra R, Keller PA. Phytochemical studies on two Australian *Anigozanthos* plant species. J Nat Prod. 2017;80(7):2141-2145. DOI: 10.1021/acs.jnatprod.7b00063.
22. Talamond P, Mondolot L, Gargadennec A, de Kochko A, Hamon S, Fruchier A, *et al*. First report on mangiferin (C-glucosyl-xanthone) isolated from leaves of a wild coffee plant, *Coffea pseudozanguebariae (*Rubiaceae*)*. Acta Bot Gallica. 2008;155(4):513-519. DOI: 10.1080/12538078.2008.10516130.
23. Hendra R, Willis A, Keller PA. Phytochemical studies on the Australian native plant species *Acacia pycnantha* and *Jacaranda mimosifolia* D. Don. Nat Prod Res. 2019;33(14):1997-2003. DOI: 10.1080/14786419.2018.1483922.
24. Slade D, Ferreira D, Marais JPJ. Circular dichroism, a powerful tool for the assessment of absolute configuration of flavonoids. Phytochemistry. 2005; 66(18):2177-2215. DOI: 10.1016/j.phytochem.2005.02.002.
25. Garo E, Wolfender JL, Hostettmann K, Hiller W, Antus S, Mavi S. Prenylated flavanones from *Monotes engleri*: on-line structure elucidation by LC/UV/NMR. Helv Chim Acta. 1998; 81(3-4):754-763. DOI: 10.1002/hlca.19980810325.
26. Friedrich W, Galensa R. Identification of a new flavanol glucoside from barley (*Hordeum vulgare L.*) and malt. Eur Food Res Technol. 2002;214:388-393. DOI: 10.1007/s00217-002-0498-x.
27. Wang Q, Pei XX, Dai X, Wang QX, Huang GZ, Cao JG. Chemical constituents of *Pyrrosia davidii* (Baker) Ching. Biochem Syst Ecol. 2023;108:104646. DOI: 10.1016/j.bse.2023.104646.
28. Burt S. Essential oils: their antibacterial properties and potential applications in foods-a review. Int J Food Microbiol. 2004; 94(3):223-253. DOI: 10.1016/j.ijfoodmicro.2004.03.022.
29. Balouiri M, Sadiki M, Saad IK. Methods for *in vitro* evaluating antimicrobial activity: A review. J Pharm Anal. 2016; 6(2):71-79. DOI: 10.1016/j.jpha.2015.11.005.
30. Uzarski JS, DiVito MD, Wertheim JA, Miller WM. Essential design considerations for the resazurin

reduction assay to noninvasively quantify cell expansion within perfused extracellular matrix scaffolds. Biomaterials. 2017;129:163-175.
DOI: 10.1016/j.biomaterials.2017.02.015.

31. Sarker SD, Nahar L, Kumarasamy Y. Microtitre plate-based antibacterial assay incorporating resazurin as an indicator of cell growth, and its application in the *in vitro* antibacterial screening of phytochemicals. Methods. 2007;42(4):321-324.
DOI: 10.1016/j.ymeth.2007.01.006.
32. Tan Z, Deng J, Ye Q, Zhang Z. The antibacterial activity of natural-derived flavonoids. Curr Top Med Chem. 2022;22(12):1009-1919.
DOI: 10.2174/1568026622666220221110506.
33. Xie Y, Yang W, Tang F, Chen X, Ren L. Antibacterial activities of flavonoids: structure-activity relationship and mechanism. Curr Med Chem. 2015; 22(1):132-149.
DOI: 10.2174/0929867321666140916113443.
34. Silhavy TJ, Kahne D, Walker S. The bacterial cell envelope. Cold Spring Harb perspect Biol. 2010; 2(5):a000414,1-16.
PMID: 20452953.
35. Nurhayati B, Singgih Wibowo M, Widyastuti Y, Putu Erawijantari P, Widowati W, Rizki Fadhil Pratama M, *et al*. *In silico* analysis of plantaricin EF that expressed by plasmid-associated bacteriocin production gene of *Lactobacillus plantarum* IBL-2 for anti-candida agent potential. Res J Microbiol. 2015; 10(12):582-591.
DOI: 10.3923/jm.2015.582.591.
36. Amer HH, Eldrehmy EH, Abdel-Hafez SM, Alghamdi YS, Hassan MY, Alotaibi SH. Antibacterial and molecular docking studies of newly synthesized nucleosides and Schiff bases derived from sulfadimidines. Sci Rep. 2021;11(1):17953,1-14.
DOI: 10.1038/s41598-021-97297-1.
37. Lee JY, Jeong KW, Shin S, Lee JU, Kim Y. Antimicrobial natural products as β-ketoacyl-acyl carrier protein synthase III inhibitors. Biorg Med Chem. 2009;17(15):5408-5413.
DOI: 10.1016/j.bmc.2009.06.059.
38. Lee JY, Lee JH, Jeong KW, Lee EJ, Kim YM. Flavonoid inhibitors of β-ketoacyl acyl carrier protein synthase III against methicillin-resistant staphylococcus aureus. Bull Korean Chem Soc. 2011;32(8):2695-2699.
DOI: 10.5012/bkcs.2011.32.8.2695.